Journal of Materials Chemistry C

RSC Publishing

PAPER

View Article Online
View Journal | View Issue

Cite this: J. Mater. Chem. C, 2013, 1, 4779

Growth of flexible N-doped SiC quasialigned nanoarrays and their field emission properties†

Shanliang Chen,[abc] Pengzhan Ying,[b] Lin Wang,[c] Guodong Wei,[c] Jinju Zheng,[c] Fengmei Gao,[c] Shubing Su[c] and Weiyou Yang*[c]

Received 22nd April 2013
Accepted 7th June 2013

DOI: 10.1039/c3tc30752b

www.rsc.org/MaterialsC

In the present work, we report the growth of flexible SiC quasialigned nanoarrays with N dopants on carbon fabric substrate *via* the catalyst-assisted pyrolysis of a polymeric precursor. The resultant products are systematically characterized by X-ray diffraction (XRD), scanning electron microscopy (SEM), high-resolution transmission electron microscopy (HRTEM) and energy-dispersive X-ray spectroscopy (EDS). The as-synthesized SiC nanowires are single-crystalline and grow along the [111] direction with a uniform spatial distribution of N dopants. The effect of the distance between the SiC array and the anode on the Field emission (FE) properties was investigated. FE measurements show that these N-doped SiC nanoarrays could be an excellent candidate for field emitters with very low turn-on fields of 1.90–2.65 V μm^{-1} and threshold fields of 2.53–3.51 V μm^{-1}, respectively, which can be mainly attributed to the decrease of work function induced by the N dopants.

1 Introduction

Field emission has been extensively investigated over the past decades.[1,2] Among the family of field emitters, flexible counterparts are attracting more and more attention due to their wide and unique applications in roll-up field emission displays, electronic textiles, large-area circuits on curved objects and so on.[3–7] One of the interesting and promising strategies for the fabrication of flexible field emitters is to directly grow low-dimensional nanostructures on flexible substrates. There are two commonly used flexible substrates for the growth of flexible emitters. One is polymers,[8–11] and the other is the carbon fabric. As compared to polymers with low melting points, carbon fabrics can endure very high temperatures with excellent thermal stability and electrical conductivity. Thus, carbon fabrics have been widely utilized as the flexible substrate for the growth of inorganic low-dimensional nanostructures under high temperatures.[12–15]

SiC nanostructures have been considered as excellent candidates for field emitters, owning to their versatile, excellent properties, such as superior mechanical properties, high thermal conductivity, low thermal-expansion coefficient, good thermal-shock resistance, as well as its excellent chemical stability and electron affinity.[16–19] Up to date, many works have focused on the field emission properties of SiC low-dimensional nanostructures, such as nanowires, nanobelts, and nanotubes. Their turn-on fields (E_{to}) under room temperature fell usually in just several or even lower than one V μm^{-1},[20–27] showing their excellent field emission properties. However, most of the reported works were based on rigid substrates (*e.g.*, graphite, silicon, and SiC wafers), which limited their applications in flexible emitters. To the best of our knowledge, few works have achieved the growth SiC low-dimensional nanostructures on flexible substrates. Wu *et al.* synthesized SiC nanowires on carbon fabrics *via* a chemical vapor deposition process and their E_{to} was 1.2–1.3 V μm^{-1}.[28,29]

Doping could be an efficient way to enhance the field emission properties of the SiC low-dimensional nanostructure, since it can significantly increase the localized density states around the Fermi energy region.[30] In the present work, for the first time, we report the synthesis of SiC nanowires (SiC-NWs) with N dopants on the carbon fabrics *via* pyrolysis of the polymeric precursor, leading to the growth of flexible N-doped SiC quasialigned nanoarrays. They exhibit a very low E_{to} and E_{thr} in the ranges of 1.90–2.84 V μm^{-1} and 2.53–3.51 V μm^{-1}, respectively, suggesting their very promising application in field emission displays.

2 Experimental procedure

The SiC-NWs with N dopants were synthesized by the catalyst-assisted pyrolysis of a polymer precursor of polysilazane (PSN,

[a]School of Chemical engineering & Technology, China University of Mining and Technology, Xuzhou City, 221116, P.R. China

[b]School of Material Science & Engineering, China University of Mining and Technology, Xuzhou City, 221116, P.R. China

[c]Institute of Materials, Ningbo University of Technology, Ningbo City, 315016, P.R. China. E-mail: weiyouyang@tsinghua.org.cn; Fax: +86-574-87081221; Tel: +86-574-87080966

† Electronic supplementary information (ESI) available: Summary of FE properties of SiC emitters and other nanostructured flexible cathodes. See DOI: 10.1039/c3tc30752b

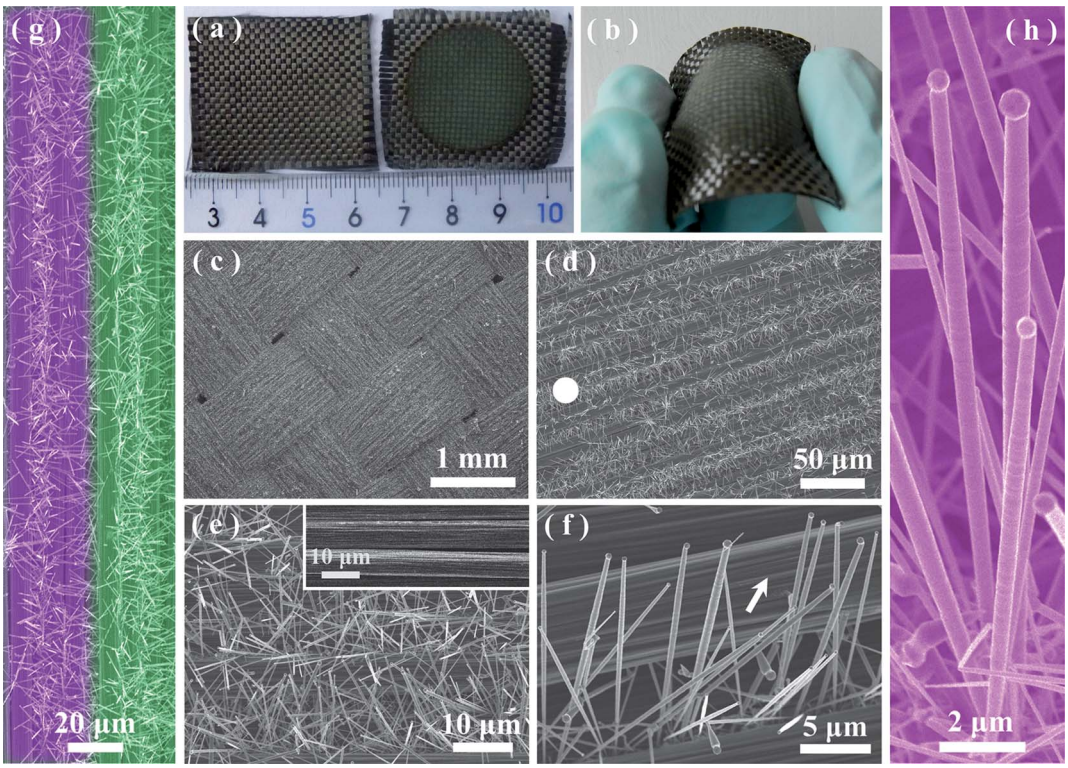

Fig. 1 (a) A typical digital photo showing the change of the carbon fabric substrates before and after pyrolysis treatment at 1500 °C. (b) The curved carbon fabric after pyrolysis. (c–f) Typical SEM images of the as-synthesized SiC quasialligned nanoarry under different magnifications. (g) A representative enlarged image showing the growth of the SiC arrays on the substrate. (h) A typical SEM image under high magnification, showing the characteristics of the grown SiC wires.

Ceraset, Kion Corporation, USA) in a graphite-heater furnace. PSN is commercially available and was used directly without further purification. Firstly, the precursor polymers were solidified by heat-treatment at 260 °C for 30 min under Ar atmosphere, and then subjected to ball-milling into powders, followed by being transferred into the bottom of a high-purity graphite crucible (purity: 99%). The substrate of carbon fabric was immersed into the ethanol solution of $Co(NO_3)_2$ with a concentration of 0.05 mol L^{-1} for 2 min, and then dried naturally in air at room temperature, and located on the top of the graphite crucible. The crucible with the substrate and the powders was placed into the graphite-heater furnace. Subsequently, an atmosphere mixture of 5 vol% nitrogen and 95 vol% argon (both are 99.99% purity, 0.1 Mpa) was introduced into the chamber. The system was evacuated to 10^{-3} Pa and then purged three times to reduce the O_2 to a negligible level. Finally, the system was heated from room temperature to 1500 °C at a rate of 30 °C min^{-1}, followed by cooling the furnace to room temperature. The whole pyrolysis process was performed under the atmosphere mixture of 5% nitrogen and 95% argon with a flow rate of 200 sccm.

The obtained products were characterized using field emission scanning electron microscopy (FESEM, S-4800, Hitachi, Japan), X-ray diffraction (XRD, D8 Advance, Bruker, Germany) with Cu Kα radiation ($\lambda = 1.5406$), and high-resolution transmission electron microscopy (HRTEM, JEM-2100F, JEOL, Japan) equipped with energy-dispersive X-ray spectroscopy (EDS, Quantax-STEM, Bruker, Germany). The measurement of the FE properties of the SiC quasialigned nanoarrays were carried out in a home-built high vacuum field emission setup with a base pressure of $\sim 3.0 \times 10^{-7}$ Pa at room temperature. The current–voltage (I–V) curves were recorded on a Keithley 248 unit. The distances between the surface of the SiC nanoarrays and the anode of the vacuum chamber were fixed at 400–800 μm.

3 Results and discussion

Fig. 1(a) shows a typical digital photo of the carbon fabric substrate before and after the pyrolysis process. The color of the carbon fabric was converted from gloss-black to greyish-green (the diameter of the greyish-green area corresponds to that of the used graphite crucible), suggesting that SiC nanostructures have been grown on the carbon fabric. The greyish-green color is distributed uniformly on the carbon fabric, implying uniform growth of the SiC nanostructures on the whole substrate. It should be noted that the carbon fabric preserves a high flexibility after the pyrolysis treatment under 1500 °C (Fig. 1(b)), since it could be strongly bended tens of times without damage in our experiments. To make a more clear observation of the structures grown on the substrates, the carbon fabric was observed under SEM, as shown in Fig. 1(c)–(h). Fig. 1(c) shows a representative SEM image under low magnification, revealing that some wire-like structures are deposited homogeneously on the whole carbon fabric substrate. The enlarged SEM images in Fig. 1(d) and (e) indicate that most of the nanowires often grow in the area between

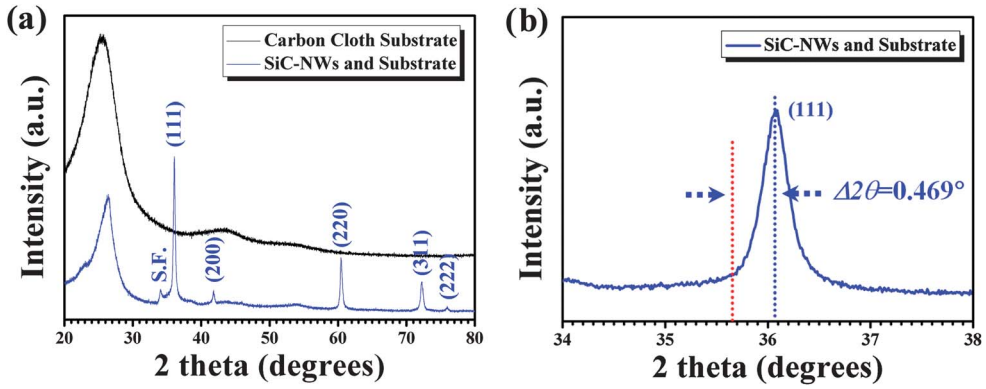

Fig. 2 (a) XRD patterns recorded from SiC-NWs + substrate and the substrate. (b) An enlarged XRD pattern showing the diffraction peak shift of the (111) crystal plane of the N-doped SiC nanoarrays.

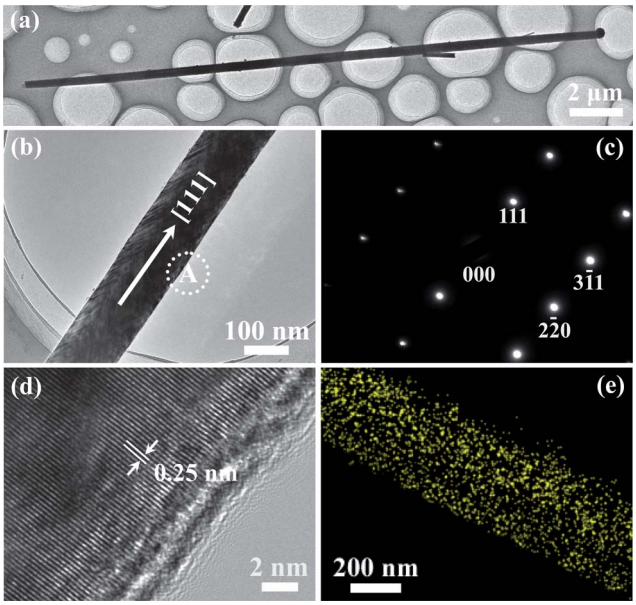

Fig. 3 (a and b) Typical TEM images of a single SiCNWs under different magnifications. (c and d) The corresponding SAED pattern and HRTEM image of the synthesized SiC-NWs. (e) A representative element mapping of the N dopants within the SiC-NWs.

two carbon fibers and usually stand vertical to the carbon fibers, which construct the nanowires into quasialigned arrays, as clearly shown in Fig. 1(g). The surface of the carbon fibers seems very smooth (shown as the marked white arrow heads in Fig. 1(f)) and similar to the original ones (as shown in the top-right inset in Fig. 1(e)). This suggests that the surfaces of the fibers maintain their condition without damage after the high temperature pyrolysis, which could favor a high flexibility of the carbon fabric to support the grown SiC quasialigned nanoarrays. The nanowires are dozens of micrometers in length and ~250 nm in diameter with a typical aspect ratio up to more than 60 (Fig. 1(h)). The surfaces of the wires are clear. The catalyst particles are often observed on the top of the nanowires (Fig. 1(h)), disclosing that the growth of the SiC-NWs is dominated by a typical vapor–liquid–solid (VLS) mechanism.

To investigate the phase compositions of the nanowires, the synthesized products were investigated by XRD. As shown in Fig. 2(a), except the diffraction of the substrates, all the other peaks can be well indexed as 3C–SiC (JCPDS Card no. 29-1129), indicating that the resultant nanowires are of only the 3C–SiC phase. The strong and sharp diffraction peaks show that the as-grown SiC-NWs possess a good crystallinity. The low intensity peak marked with "SF" is attributed to the stacking faults in the 3C–SiC wires.[31] Fig. 2(b) presents a closer examination of the (111) peak of the XRD patterns. Compared with the standard data (JCPDS Card no. 29-1129), which is marked as the red dashed line, the (111) peak of the synthesized 3C–SiC nanowires shifts to a higher angle with a 2θ of 0.469°. The calculated lattice parameter of a shows a 1.26% decrease as compared to that of pure 3C–SiC. In line with our previous work,[32] it can be confirmed that the SiC nanowires were successfully doped by the N atoms.

Further characterization of the obtained SiC quasialigned nanoarrays was carried out using TEM. Fig. 3(a) and (b) are typical TEM images of the nanowires under various magnifications, suggesting the nanowires were averagely sized at ~250 nm in diameter with a smooth surface, which was consistent with the SEM observations. Fig. 3(c) is the corresponding selected area electron diffraction (SAED) pattern recorded from the marked area of *A* of a single nanowire, which can be indexed to the 3C–SiC (JCPDS Card no. 41-0360). The SAED pattern is identical over the entire nanowire, suggesting its single-crystalline nature. Fig. 3(d) presents a representative HRTEM image of the as-synthesized nanowires. The interplanar spacing d of two neighboring lattice fringes is ~0.25 nm, fitting the {111} plane distance of 3C–SiC. Both the SAED pattern and the HRTEM image suggest that the SiC-NWs grew along the [111] direction, as indexed in Fig. 3(b). Fig. 3(e) shows a typical element mapping N of a single wire, suggesting the uniform spatial distribution of N dopants within the SiC nanowires. The concentration of N dopants detected under TEM was ~2.38 at.% (experimental setup is not shown here).

The field emission characteristics of the resultant N-doped SiC quasialigned nanoarrays were revealed by emission current density (J) *versus* the applied electric field (E) plot. Fig. 4(a)

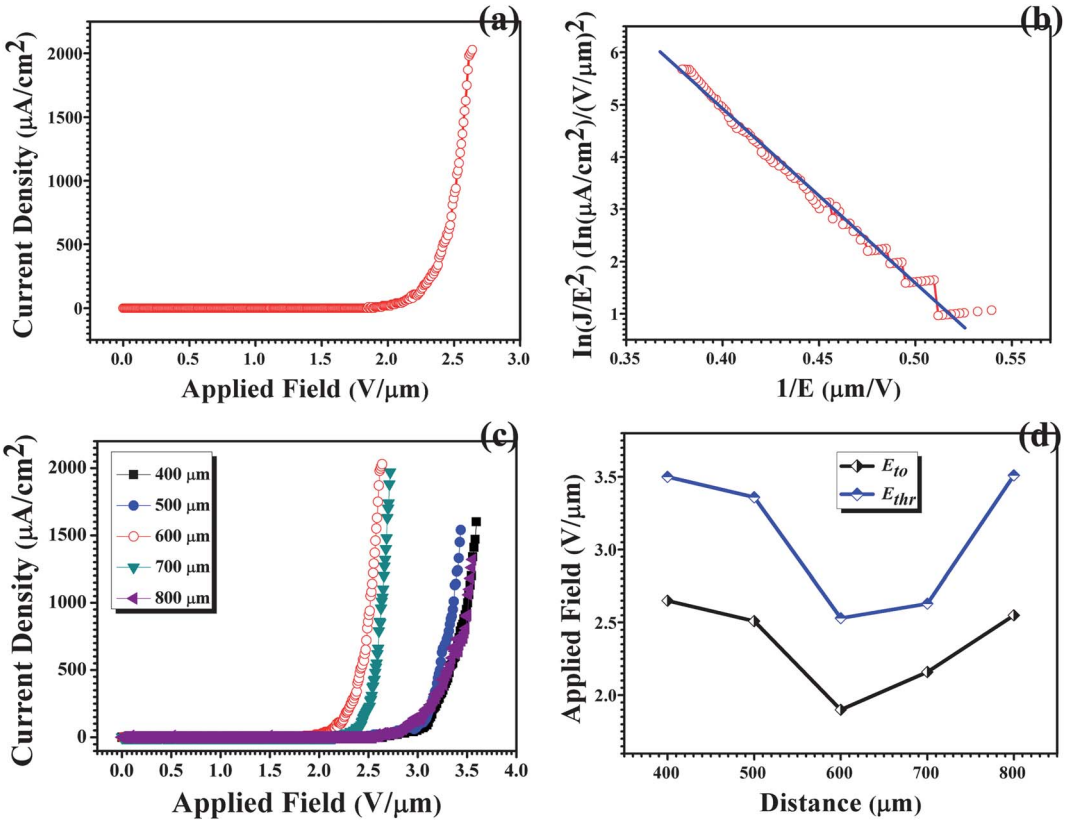

Fig. 4 (a and b) A typical *J–E* curve and corresponding F–N plot of the N-doped SiC nanoarrays with a *d* fixed at 600 μm. (c) Typical *J–E* curves of the N-doped SiC nanoarrays with *d* fixed at 400–800 μm. (d) The variation of E_{to} and E_{thr} with *d*.

shows the FE current densities *versus* the applied electric fields (*J–E*) plot of the N-doped SiC nanoarrays with *d* (the distance between the surface of SiC-NWs and the anode) fixed at 600 μm. The *J–E* curve was obtained after sweeping the voltage several times until the electron emission was stable. The relatively smooth and consistent curves indicate their stable electron emission. The turn-on field (E_{to}, defined to the electric field required to produce a current density of 10 μA cm^{-2}) and the threshold field (E_{thr}, defined to the electric field required to produce a current density of 1 mA cm^{-2}) were 1.90 V μm^{-1} and 2.53 V μm^{-1}, respectively. These values are lower than those in most of the reported works on SiC nanostructure-based emitters, as well as the other nanostructure-based flexible emitters (ESI, Table S1†). To understand the FE behavior, the *J–E* data has been analyzed by the FN equation:[33]

$$J = (A\beta^2E^2/\Phi)\exp[-B\Phi^{3/2}(\beta E)^{-1}] \quad (1)$$

where *J* is the emission current density, *E* is the applied field, Φ is the work function, *A* and *B* are constants, and β is the field enhancement factor. The corresponding F–N plot, obtained by plotting $\ln(J/E^2)$ *versus* $1/E$, is depicted in Fig. 4(b). The slope of the F–N plot shows an approximately linear relationship, suggesting that the electron emission from the SiC nanoarrays follows the conventional field emission mechanism. By taking the work function of 4.0 eV for SiC under room temperature,[19] the field enhanced factor β was calculated to be 1710. Fig. 4(c) shows the *d*-dependent field emission properties of the as-synthesized flexible N-doped SiC nanoarrays, in which *d* was fixed between 400 and 800 μm with an interval distance of 100 μm. The E_{to} and E_{thr} were in the range of 1.90–2.65 V μm^{-1} and 2.53–3.51 V μm^{-1} (Fig. 4(d)), respectively. It seems that the *d* value has a notable effect on the field emission performance of the N-doped SiC nanoarrays. With the increase of *d*, the E_{to} and E_{thr} decreased first, and then increased. When *d* was set as 600 μm, the best FE properties were reached. That is to say, in the current experiment, the flexible N-doped SiC nanoarrays exhibited the best FE properties with a fixed distance of 600 μm between the arrays and the anodes. We propose this might be attributed to the following two facts: (i) one is that the direction of the emitted electrons from the SiC quasialigned nanoarrays were not always perpendicular to the anode. (ii) The other is that various *d* will result in different electric fields ($E = V/d$) between the anode and emitter. Thus, with respect to the constant area of the anode, various *d* might make anodes with different capabilities to capture the electrons escaped from the nanostructures, leading to the *d*-dependent FE properties of the SiC nanoarrays. The detailed mechanism needs to be further investigated.

Considering the relatively low density growth (Fig. 1(d) and (g)) and the large diameter size (~250 nm) of the nanowires with catalytic droplets on the tips (the alloy drops could limit the electron emission and reduce the current density[34,35]), we attribute the excellent FE properties of the current SiC nanoarrays mainly to the successful N doping of the nanowires. The

N-doped SiC nanowires mainly form substitutional solid solutions by the substitution of N to C,[32] which could result in the increase of the effective density of electrons state (N_v) of SiC. The relationship between the Fermi energy (E_F) and N_v can be expressed as the following equation:[36]

$$E_F = \frac{(E_C + E_V)}{2} + \left(\frac{k_B T_L}{2}\right)\ln\left(\frac{N_V}{N_C}\right) \quad (2)$$

where E_C and E_V refer to the respective energies of the conduction and valence band, K_B is the Boltzmann constant, T_L is the lattice temperature, N_V and N_C are the effective density of electrons and holes state, respectively. For the N-doped SiC-NWs, the first term and the N_C in the second term of eqn (2) are constants. Thus, the increase of N_V in SiC induced by the N dopants could lead to a higher E_F. The relationship between E_F and the work function Φ can be defined as the following equation:[37]

$$\Phi = E_0 - E_F \quad (3)$$

where the E_0 and E_F are the vacuum level and the Fermi energy level, respectively. This equation implies that a higher E_F could result in a smaller Φ, which favors a better FE performance.[11,38–40] Briefly, the N dopants within SiC would increase the effective density of electrons state and reduce the work function, which consequently facilitate an excellent FE performance of the present N-doped SiC nanoarrays.

4 Conclusions

In summary, we have demonstrated the growth of flexible N-doped SiC quasialigned nanoarrays with N dopants on a carbon fabric substrate *via* the pyrolysis of polymeric precursor with $Co(NO_3)_2$ as the catalyst. The as-synthesized SiC nanowires are single-crystalline and grow along the [111] direction with a uniform spatial distribution of N dopants. The distance between the SiC array and the anode play a notable effect on their FE properties. The N-doped SiC nanoarrays exhibit very low turn-on fields of 1.90–2.65 V μm^{-1} and threshold fields of 2.53–3.51 V μm^{-1}, respectively, which can be mainly attributed to the decrease of work function induced by the N dopants. The field enhanced factor is calculated to be 1710. The current work suggests that these flexible N-doped SiC nanoarrays could be an excellent candidate for field emitters, which are promising for utilization in field emission displays and other electronic nanodevices.

Acknowledgements

This work was supported by the 973 program (Grant no. 2012CB326407), National Natural Science Foundation of China (NSFC, Grant no. 51072084, 51002083 and 51202115), Zhejiang Provincial Science Foundation for Distinguished Young Scholars (Grant no. R4100242), Zhejiang Provincial Natural Science Foundation of China (ZJNSFC, Grant no. Y4110529), and Natural Science Foundation of Ningbo Municipal Government (Grant no. 2011B1009, 2011A610182 and 2011A610097).

References

1 L. Li, P. Wu, X. Fang, T. Zhai, L. Dai, M. Liao, Y. Koide, H. Wang, Y. Bando and D. Golberg, *Adv. Mater.*, 2010, **22**, 3161.
2 L. Li, Y. Zhang, X. Fang, T. Zhai, M. Liao, X. Sun, Y. Koide, Y. Bando and D. Golberg, *J. Mater. Chem.*, 2011, **21**, 6525.
3 T. Georgiou, R. Jalil, B. D. Belle, L. Britnell, R. V. Gorbachev, S. V. Morozov, Y. J. Kim, A. Gholinia, S. J. Haigh and O. Makarovsky, *Nat. Nanotechnol.*, 2012, **8**, 100.
4 H. Zhou, J. H. Seo, D. M. Paskiewicz, Y. Zhu, G. K. Celler, P. M. Voyles, W. Zhou, M. G. Lagally and Z. Ma, *Sci. Rep.*, 2013, **3**, 1291.
5 I. Lahiri, V. P. Verma and W. Choi, *Carbon*, 2011, **49**, 1614.
6 P. Ghosh, M. Z. Yusop, S. Satoh, M. Subramanian, A. Hayashi, Y. Hayashi and M. Tanemura, *J. Am. Chem. Soc.*, 2010, **132**, 4034.
7 T. Tan, H. Sim, S. Lau, H. Yang, M. Tanemura and J. Tanaka, *Appl. Phys. Lett.*, 2006, **88**, 103105.
8 C. Y. Lee, S. Y. Li, P. Lin and T. Y. Tseng, *J. Nanosci. Nanotechnol.*, 2005, **5**, 1088.
9 B. J. Yoon, E. H. Hong, S. E. Jee, D. M. Yoon, D. S. Shim, G. Y. Son, Y. J. Lee, K. H. Lee, H. S. Kim and C. G. Park, *J. Am. Chem. Soc.*, 2005, **127**, 8234.
10 J. H. Deng, R. T. Zheng, Y. M. Yang, Y. Zhao and G. A. Cheng, *Carbon*, 2012, **50**, 4732.
11 H. J. Jeong, H. D. Jeong, H. Y. Kim, S. H. Kim, J. S. Kim, S. Y. Jeong, J. T. Han and G. Lee, *Small*, 2012, **8**, 9.
12 B. Zeng, G. Xiong, S. Chen, W. Wang, D. Wang and Z. Ren, *Appl. Phys. Lett.*, 2007, **90**, 033112.
13 S. Jo, D. Wang, J. Huang, W. Li, K. Kempa and Z. Ren, *Appl. Phys. Lett.*, 2004, **85**, 810.
14 D. Banerjee, S. H. Jo and Z. F. Ren, *Adv. Mater.*, 2004, **16**, 2028.
15 T. T. Baby and S. Ramaprabhu, *Appl. Phys. Lett.*, 2011, **98**, 183111.
16 J. B. Casady and R. W. Johnson, *Solid-State Electron.*, 1996, **39**, 1409.
17 E. W. Wong, P. E. Sheehan and C. M. Lieber, *Science*, 1997, **277**, 1971.
18 J. Fan, X. Wu and P. K. Chu, *Prog. Mater. Sci.*, 2006, **51**, 983.
19 X. Fang, Y. Bando, U. Gautam, C. Ye and D. Golberg, *J. Mater. Chem.*, 2008, **18**, 509.
20 Y. Yang, G. Meng, X. Liu, L. Zhang, Z. Hu, C. He and Y. Hu, *J. Phys. Chem. C*, 2008, **112**, 20126.
21 G. Yang, H. Cui, Y. Sun, L. Gong, J. Chen, D. Jiang and C. Wang, *J. Phys. Chem. C*, 2009, **113**, 15969.
22 G. Shen, Y. Bando and D. Golberg, *Cryst. Growth Des.*, 2007, **7**, 35.
23 H. Cui, Y. Sun, G. Yang, J. Chen, D. Jiang and C. Wang, *Chem. Commun.*, 2009, 6243.
24 M. G. Kang, H. J. Lezec and F. Sharifi, *Nanotechnology*, 2013, **24**, 065201.
25 S. Deng, Z. Li, W. Wang, N. Xu, J. Zhou, X. Zheng, H. Xu, J. Chen and J. She, *Appl. Phys. Lett.*, 2006, **89**, 023118.
26 C. Tang and Y. Bando, *Appl. Phys. Lett.*, 2003, **83**, 659.

27 Z. Pan, H. L. Lai, F. C. Au, X. Duan, W. Zhou, W. Shi, N. Wang, C. S. Lee, N. B. Wong and S. T. Lee, *Adv. Mater.*, 2000, **12**, 1186.
28 R. Wu, K. Zhou, J. Wei, Y. Huang, F. Su, J. Chen and L. Wang, *J. Phys. Chem. C*, 2012, **116**, 12940.
29 R. Wu, K. Zhou, X. Qian, J. Wei, Y. Tao, S. Chorng Haur, L. Wang and Y. Huang, *Mater. Lett.*, 2013, **91**, 220.
30 X. Zhang, Y. Chen, Z. Xie and W. Yang, *J. Phys. Chem. C*, 2010, **114**, 8251.
31 K. Koumoto, S. Takeda, C. Pai, T. Sata and H. Yanagida, *J. Am. Ceram. Soc.*, 1989, **72**, 1985.
32 Z. He, L. Wang, F. Gao, G. Wei, J. Zheng, X. Cheng, B. Tang and W. Yang, *CrystEngComm*, 2013, **15**, 2354.
33 R. Fowler and L. Nordheim, *Proc. R. Soc. London, Ser. A*, 1928, **119**, 173.
34 W. A. De Heer, A. Chatelain and D. Ugarte, *Science*, 1995, **270**, 1179.
35 W. Zhu, G. Kochanski and S. Jin, *Science*, 1998, **282**, 1471.
36 S. M. Sze and K. K. Ng, *Physics of semiconductor devices*, Wiley-interscience, 3rd edn, 2006.
37 M. Fransen, T. L. Van Rooy and P. Kruit, *Appl. Surf. Sci.*, 1999, **146**, 312.
38 K. Y. Chun, H. S. Lee and C. J. Lee, *Carbon*, 2009, **47**, 169.
39 U. K. Gautam, L. Panchakarla, B. Dierre, X. Fang, Y. Bando, T. Sekiguchi, A. Govindaraj, D. Golberg and C. Rao, *Adv. Funct. Mater.*, 2009, **19**, 131.
40 G. Wei, H. Liu, C. Shi, F. Gao, J. Zheng, G. Wei and W. Yang, *J. Phys. Chem. C*, 2011, **115**, 13063.